JOURNAL OF VIROLOGY, June 1988, p. 2164–2172
0022-538X/88/062164-09$02.00/0

Vol. 62, No. 6

Functional and Topographical Analyses of Epitopes on the Hemagglutinin (VP4) of the Simian Rotavirus SA11

JOHN W. BURNS,[1] HARRY B. GREENBERG,[2] ROBERT D. SHAW,[2]† AND MARY K. ESTES[1,3]*

Departments of Virology and Epidemiology[1] and Medicine,[3] Baylor College of Medicine, Houston, Texas 77030, and Department of Medicine, Division of Gastroenterology, Stanford University School of Medicine, Stanford, California 94305[2]

Received 22 October 1987/Accepted 8 March 1988

An immunochemical analysis of the hemagglutinin (VP4) of the simian rotavirus SA11 was performed to better understand the structure and function of this molecule. Following immunization of mice with double-shelled virus particles and VP4-enriched fractions from CsCl gradients, a battery of anti-SA11 hybridomas was generated. A total of 13 clones secreting high levels of anti-VP4 monoclonal antibody (MAb) was characterized and compared with two cross-reactive anti-VP4 MAbs generated against heterologous rhesus (RRV) and porcine (OSU) rotavirus strains. These cross-reactive MAbs effectively neutralized SA11 infectivity in vitro. The epitopes recognized by these 15 MAbs were grouped into six antigenic sites on the SA11 hemagglutinin. These sites were identified following analysis of the MAbs by using a simple competitive binding enzyme-linked immunosorbent assay (ELISA) and biological assays. Three of the antigenic sites were involved in neutralization of virus infectivity in vitro. All the MAbs with neutralization activity and two nonneutralizing MAbs were able to inhibit viral hemagglutination of human erythrocytes. Competitive binding ELISA data showed a positive cooperative binding effect with some pairs of the anti-VP4 MAbs, apparently due to a conformational change induced by the binding of the first MAb. Some of the MAbs also bound better to trypsin-treated virus than to non-trypsin-treated virus. A topographic map for VP4 is proposed on the basis of the observed properties of each antigenic site.

Rotavirus infections are clearly associated with infantile gastroenteritis, and reports of disease in adults are now appearing more frequently (9, 16, 25, 26). Recognition that these viruses are significant pathogens that infect numerous mammalian and avian species, including humans, has stimulated research directed at developing effective methods of disease prevention and control (16, 21).

The rotaviruses, members of the *Reoviridae*, are nonenveloped double-shelled particles that possess a genome of 11 segments of double-stranded RNA. The RNA segments are contained within a core particle that, in the simian rotavirus SA11, is composed of VP1, a 125,000-molecular-weight (125K) protein, VP2 (94K), and the recently identified genome segment 3 protein, named VP3 (88K) (29a). The inner capsid is composed solely of VP6 (41K) and surrounds the core particle. The outer capsid contains at least three structural proteins: VP4 (88K), the hemagglutinin that is encoded by genome segment 4, and VP7[1] and VP7[2] (38K), two glycoproteins encoded by genome segment 9 (4, 15, 16). The genome segment 4 protein was previously called VP3 but was renamed VP4 when the protein encoded by genome segment 3 was identified as a structural protein (29a).

Viral infectivity in vitro is greatly enhanced by proteolytic cleavage of VP4, resulting in the formation of VP5* (60K) and VP8* (28K) (11, 14). A number of other biological activities, e.g., adaptation of virus to growth in tissue culture (18), induction of neutralizing antibodies, and determination of virulence in vivo (19, 23, 35–37), have been associated with VP4. Administration of at least one anti-VP4 monoclonal antibody (MAb) can also provide passive protection against virus challenge in a murine model of rotavirus infection (38).

An epitope map for the outer capsid glycoprotein (VP7) of SA11 has been published previously (41). In contrast, little is known about the antigenic topography of the SA11 hemagglutinin, although some epitopes on VP4 of a rhesus rotavirus (31, 40) and a human rotavirus (43) have been characterized. Detailed knowledge of the immunological and biological properties of the rotavirus outer capsid proteins should facilitate evaluation of the occurrence and biological significance of antigenic variation among these viruses (6, 22). Further, identification of neutralizing antigenic sites may prove useful in the development of an effective rotavirus vaccine. This paper reports the characterization and use of a new battery of MAbs to analyze the simian rotavirus SA11 hemagglutinin. We have chosen SA11 because it has been the most extensively studied rotavirus strain, it can be propagated to high titers in vitro, and it is considered to be the prototype virus of serotype 3 (16).

MATERIALS AND METHODS

Virus production and purification and radiolabeled lysates. SA11 was propagated in MA104 cells grown in 850-cm^2 roller bottles. Stocks of virus were generated at a low multiplicity of infection (MOI) in medium 199 containing 2 μg of trypsin per ml. For virus preparations generated in the absence of trypsin, MOIs of 20 to 40 PFU per cell were used. Infection was allowed to proceed until at least 80% of the cells showed cytopathic effects. The roller bottles were then freeze-thawed three times, and the resulting lysate was sonicated. Such preparations were used as the antigens for hemagglutination inhibition (HI) and enzyme-linked immunosorbent assay (ELISA). Virus was cultivated at a high MOI and was purified by using CsCl density gradients as described previously (14).

* Corresponding author.
† Present address: Department of Medicine, Division of Gastroenterology, State University of New York at Stony Brook, Stony Brook, NY 11794.

Radiolabeled, virus-infected cell lysates were prepared in stationary cultures of confluent MA104 monolayers by using an MOI of 25 PFU per cell and 25 μCi of [^{35}S]methionine per ml (Amersham Corp., Arlington Heights, Ill.). Labeled lysates were solubilized in a solution containing 20 mM Tris hydrochloride (pH 9.0), 137 mM NaCl, 1 mM $CaCl_2$, 0.5 mM $MgCl_2$, 1% Nonidet P-40, 2% aprotinin, 10% glycerol, and 2 mM phenylmethylsulfonyl fluoride for use in the solid-phase immunoisolation technique (SPIT) or in RIPA buffer for direct immunoprecipitation as previously described (4).

Generation of hybridomas. Female BALB/c mice were initially immunized intraperitoneally with purified double-shelled SA11 particles. This viral immunogen was generated in the presence of trypsin and emulsified in an equal volume of Freund complete adjuvant. The mice were boosted intraperitoneally 1 month later with the same viral preparation in Freund incomplete adjuvant. After 4 months, a mixture of purified double-shelled particles and proteins isolated from the top fractions of CsCl gradients was injected intraperitoneally. After extensive dialysis against 0.01 M phosphate-buffered saline (pH 7.2) (PBS), this antigen mixture was administered 6, 4, 3, and 2 days prior to fusion with P3X63 Ag8.653 myeloma cells. On days 3 and 2 prior to fusion, the immunogen was given both intraperitoneally and intravenously.

After fusion with polyethylene glycol (29), the cells were suspended in Dulbecco minimal essential medium containing 2% Ewing sarcoma growth factor (Costar Europe Ltd., Badhoevedorp, The Netherlands) and 20% fetal bovine serum (complete medium). For the first 2 weeks, HAT (hypoxanthine-aminopterin-thymidine; Sigma Chemical Co., St. Louis, Mo.) was included in the medium. Viable hybrids were initially screened using a micro-immunofluorescence (micro-IF) procedure. Positive cultures were subcloned at least twice by limiting dilutions and then expanded for further characterization and ascites production. The protein specificity of each hybridoma was determined by analyzing the reactivity of supernatant (and later ascites) fluids in immunoprecipitation (4) or SPIT (described below), with [^{35}S]methionine-labeled, SA11-infected cell lysates. The isotype of individual MAbs was determined by using the MonoAb-ID EIA isotyping kit (Zymed Laboratories, South San Francisco, Calif.).

Micro-IF tests. Confluent monolayers of MA104 cells were grown in 96-well plates (Costar, Cambridge, Mass.). The monolayers were gently washed twice with PBS and then infected with virus at a high MOI in medium 199 without trypsin. After an overnight incubation at 37°C with 5% CO_2, the medium was removed, the cells were fixed with 100% ethanol, and the plates were stored at −20°C. Before use, the infected-cell monolayers (micro-IF plates) were rehydrated with PBS.

The micro-IF test was used to screen viable hybrids when large colonies had grown out. From each well containing hybrid cells, 50 μl of supernatant fluid was transferred into wells of a micro-IF plate and incubated at 37°C for 30 min. The micro-IF plates were washed three times with PBS, and fluorescein-conjugated goat anti-mouse immunoglobulin (G, M, and A) antibody (Organon Teknika, Malvern, Pa.) was added. The plates were incubated for an additional 30 min at 37°C, washed three times with PBS, and examined by fluorescence microscopy.

This micro-IF procedure also was used to determine cross-reactivity with heterologous rotavirus strains. For this purpose, MA104 monolayers were infected with different group A rotaviruses at low MOIs. After an overnight incubation and ethanol fixation, immunoglobulin purified by high-performance liquid chromatography (HPLC) was tested at a concentration of 4 μg/ml in PBS. The remainder of the procedure was carried out as described above.

SPIT. This technique, originally described by Tamura et al. (42), was used to determine the polypeptide specificities of the hybridomas. We initially identified MAb specificity by an indirect technique and later verified these results by a direct technique.

For the indirect procedure, polyvinyl chloride microplates were coated overnight at room temperature with 5 μg of goat anti-mouse immunoglobulin (immunoglobulin G [IgG] and IgM; Tago, Inc., Burlingame, Calif.) in carbonate-bicarbonate buffer (pH 9.6) per well. The plates were then blocked with bovine lacto transfer technique optimizer (BLOTTO; 27) for 2 h at 37°C and were washed once with PBS containing 0.05% Tween 20 (PBS-T); hybridoma supernatant fluid was added and allowed to bind by incubating overnight at 4°C. The plates were washed with PBS-T, and a [^{35}S]methionine-labeled lysate was added to each well. After an overnight incubation at 4°C, the lysate was removed and the plates were washed three times with PBS containing 0.01% sodium dodecyl sulfate (SDS), 0.1% sodium deoxycholate, 1% Nonidet P-40, and 1 mM sodium azide. Bound proteins were removed by using SDS-polyacrylamide electrophoresis sample buffer (1% SDS, 10% 2-mercaptoethanol, 0.5 M urea, 0.05 M Tris hydrochloride [pH 6.8], 10% glycerol, 0.0025% phenol red). The samples were boiled for 2 min and then analyzed by electrophoresis on 10% polyacrylamide gels containing 0.001% SDS. The gels were fixed in 25% methanol–7% acetic acid, soaked for 1 to 2 h in autoradiographic image enhancer (Autofluor; National Diagnostics, Somerville, N.J.), and dried prior to applying them to X-ray film (X-Omat; Eastman Kodak Co., Rochester, N.Y.).

For the direct test, radiolabeled lysate was added to polyvinyl chloride plates coated directly with 2 μg of HPLC-purified immunoglobulin per ml and blocked as described above. The bound proteins were removed and analyzed as described above.

PRN and HI assays. Plaque reduction neutralization (PRN) assays were carried out using approximately 40 PFU per well in 6-well plates (Costar) as previously described (13). Serial 10-fold dilutions of ascites fluids were used, starting at a dilution of 1:40.

HI assays were performed in 96-well microtiter plates by using serial twofold dilutions of HPLC-purified immunoglobulin (starting at 40 μg/ml) in PBS containing 0.3% bovine serum albumin. Virus was diluted in PBS–0.3% bovine serum albumin to contain 4 hemagglutination units in 25 μl. The virus-MAb mixtures were incubated at 37°C for 30 min, and then 50 μl of 0.5% human type O erythrocytes in PBS was added. Results of the test were read after 1 h at room temperature.

HPLC purification of MAbs from ascites fluids. Ascites fluid was generated by inoculating pristane (Aldrich Chemical Co., Milwaukee, Wis.)-primed BALB/c mice intraperitoneally with 6×10^5 to 3×10^6 cells (3). Ascites fluid was diluted 1:3 in 10 mM MES [2-(*N*-morpholino)ethanesulfonic acid] (pH 5.6) (Calbiochem-Behring, San Diego, Calif.) and filtered sequentially through a 0.8-μm-pore-size Millex-PF filter and then a 0.22-μm-pore-size Millex-GV low-binding filter (Millipore Corp., Bedford, Mass.) before being applied to a Bakerbond ABx HPLC column equilibrated with 10 mM MES (J. T. Baker Chemical Co., Phillipsburg, N.J.). The column was subsequently eluted with a linear 0 to 50%

gradient of 500 mM $(NH_4)_2SO_4$ in 10 mM sodium acetate (J. T. Baker Chemical Co.) as described previously (33). All buffers contained 0.01% sodium azide. Peaks eluted from the column were analyzed by SDS-polyacrylamide gel electrophoresis (10% polyacrylamide) to determine the location of the purified immunoglobulin. Protein concentrations of the eluted immunoglobulin peaks were determined by the dye-binding assay of Bradford (2). Stock solutions (50 μg/ml) were prepared by using 10 mM MES. These stock solutions were stored at 4°C and used for all of the MAb procedures, except neutralization tests.

Epitope mapping. Epitope mapping was performed using a competitive MAb capture ELISA (CMCE) previously described (20). This assay was performed by coating the wells of polyvinyl chloride microtiter plates with 60 μl (2 μg/ml) of HPLC-purified immunoglobulin in carbonate-bicarbonate buffer (pH 9.6). The plates were incubated overnight at room temperature and were then blocked with BLOTTO for at least 2 h at 37°C.

At the same time, we incubated limiting amounts of antigen (diluted in PBS) in separate tubes with 5, 1, 0.5, 0.1, and 0.05 μg of competitor MAb per ml overnight at room temperature. The competing MAb was either a heterologous MAb or the same MAb used to coat the microtiter plate (HPLC-purified immunoglobulin was used for both capture and competitor MAb in all tests). The antigen-antibody complexes were added to wells of blocked plates containing the capture MAb and were incubated for at least 4 h at 37°C. The plates were washed three times with PBS-T, hyperimmune rabbit anti-rotavirus serum was added, and the plates were incubated for 2 h at 37°C. After an additional three washes with PBS-T, horseradish peroxidase-conjugated goat anti-rabbit IgG antibody (HyClone Laboratories, Logan, Utah) was added and the plates were incubated for 1 h at 37°C. The plates were again washed three times with PBS-T, and ABTS [2,2'azinobis(3-ethylbenzthiazoline sulfonic acid); Sigma Chemical Co.] was added. After a 30-min incubation at room temperature, optical densities were determined at 414 nm with a Titertek Multiskan plate reader (Flow Laboratories, Inc., McLean, Va.).

MCE. MAb capture ELISA (MCE) was performed exactly as the CMCE, except the competitive step involving preincubation of the antigen with the competing MAb was omitted.

RESULTS

Generation of MAbs to SA11 VP4. A battery of anti-VP4 MAbs was generated to begin an analysis of the SA11 hemagglutinin. To increase the likelihood of obtaining MAbs reactive with VP4, we immunized mice with a mixture of double-shelled particles purified on CsCl gradients and soluble viral proteins found in the top fractions of these gradients. Figure 1 shows a typical CsCl gradient profile (A) and the polyacrylamide gel analysis of fractions from this gradient (B). The top fraction is enriched in VP4 as compared with those fractions containing double-shelled particles. By this protocol, over 20 hybridomas reactive with VP4 of SA11 were generated from a single fusion. A total of 13 of these hybridomas was chosen for further characterization and comparative studies, along with two cross-reactive anti-VP4 MAbs made to heterologous viruses (954/23, anti-RRV [19]; 2G4, anti-OSU [40]).

A summary of the properties of these 15 MAbs analyzed in our studies is shown in Table 1. Six of these hybridomas (8B6, 9F6, 7G6, 10G6, 2G4, and 954/23) showed neutralizing

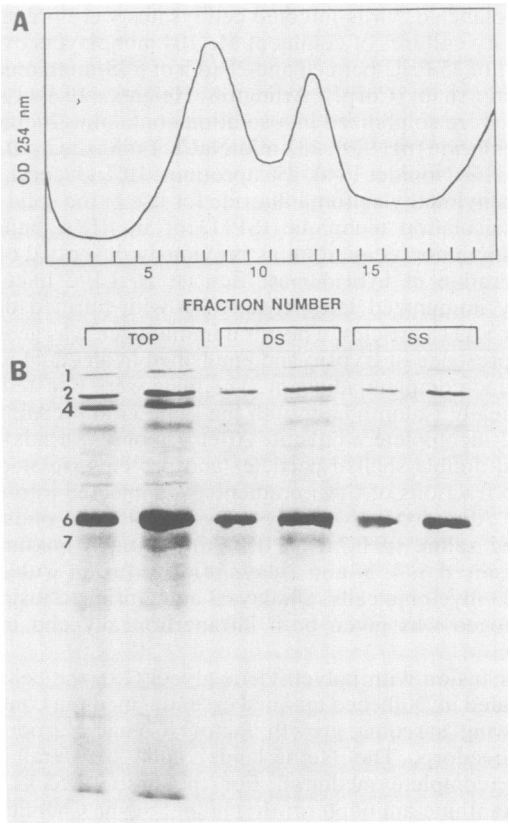

FIG. 1. SA11 double-shelled (DS) and single-shelled (SS) particles were purified by Genetron extraction, followed by banding in CsCl gradients, and 0.2-ml fractions were collected. (A) Tracing of optical density at 254 nm for a typical gradient. The three major peaks are fraction 1 (top fraction), fractions 5 through 10 (double-shelled particles; 1.36 g/ml), and fractions 12 through 14 (single-shelled particles; 1.38 g/ml). (B) Silver staining of the proteins found in each peak in a 10% polyacrylamide gel. Two different volumes (7 and 15 μl) of the pooled material under each peak were analyzed. Numbers at the left indicate the viral polypeptides, as designated by Estes et al. (16) and modified by Liu et al. (29a).

activity with SA11 in PRN tests. HI tests were performed with purified IgG because of differences observed in the antibody titers of different hybridomas and differences between ascites fluids from different mice given the same hybridoma (unpublished observation; 3, 32). All the MAbs with neutralizing activity possessed HI activity. All HI-positive MAbs showed HI cross-reactivity with two other serotype 3 viruses (RRV and CU-1 strains), although the highest titers were usually observed with SA11 (data not shown). MAbs without neutralizing activity lacked HI activity or had low HI titers (8D4 and 9E3).

The polypeptide specificities of the MAbs were determined using the SPIT. Initial attempts to identify protein specificities using radioimmunoprecipitation suggested this technique was not entirely reliable with anti-VP4 or anti-VP7 MAbs (personal observations; 41). In contrast, SPIT was found to be a reliable technique when using either hybridoma supernatant or ascites fluids. For example, MAbs 10G6 and 7G6 failed to react with any proteins by radioimmunoprecipitation but clearly reacted with VP4 in the SPIT; 9F6 reacted positively in both assays, as did 2G4. However, using 2G4 in the radioimmunoprecipitation procedure, we consistently

TABLE 1. Summary of properties of anti-VP4 MAbs

MAb	Isotype	Neutralization titer with SA11[a]	HI activity with SA11[b]	Site assigned
3C8	IgG2a	<40	− (40)	NN1[c]
5B5	IgG2a	<40	− (40)	NN1
5E4	IgG2a	<40	− (40)	NN1
7C6	IgG2a	<40	− (40)	NN1
1D8	IgG2a	<40	− (40)	NN2
5B10	IgG2a	<40	− (40)	NN2
8D4	IgG2b	<40	+ (40)	NN2
9E3	IgG1	<40	+ (40)[d]	NN2
3D8	IgG2a	<40	− (40)	NN3
8B6	IgG1	4,000	+ (1.25)	NP1a
9F6	IgG1	4,000	+ (1.25)	NP1a
7G6	IgG2b	40,000	+ (0.08)	NP1b
10G6	IgG1	400,000	+ (0.08)	NP1b
2G4	IgG1	40,000	+ (0.08)	NP2
954/23	IgG1	400	+ (0.08)	NP3

[a] Neutralization titer is the reciprocal of the dilution of ascites fluid that caused a 60% reduction in 30 to 40 plaques with SA11 plated on MA104 monolayers. All MAbs were generated to SA11, except 2G4 and 954/23 (generated to OSU and RRV rotaviruses, respectively). Neutralization titers for the 954/23 and 2G4 MAbs with their homologous viruses were both >40,000.

[b] HI titers were determined for all MAbs by using SA11 stock solutions generated in the presence of trypsin. HPLC-purified IgG was used as described in Materials and Methods, starting at 40 μg/ml. The results show the concentration of purified immunoglobulin at the lowest concentration tested (if negative) or at the final concentration with reactivity (if positive).

[c] Antigenic site assignments were based on biological properties (neutralization and HI titers) and epitope mapping studies (see Fig. 3 and 4). NN, Neutralization-negative MAbs; NP, neutralization-positive MAbs.

[d] A HI titer of 1:160 was obtained with SA11 by using 9E3 ascites fluid.

observed the coprecipitation of both VP4 and VP6. Figure 2 shows typical reactivities of some of the MAbs tested by using the direct SPIT.

Cross-reactivity of the MAbs with heterologous virus strains was also assayed by micro-IF tests (Table 2). All the rotavirus strains tested, except S2, showed reactivity with the NN2 MAbs (8D4 and 9E3). The other nonneutralizing MAbs reacted with several different rotavirus strains. The NP2 MAb, 2G4, reacted with both the serotype 3 rotaviruses and the serotype 8 rotavirus 69M. This MAb has previously been reported to be broadly cross-reactive. The NP1 and NP3 MAbs reacted only with serotype 3 viruses by micro-IF, and the NP1a and NP3 MAbs reacted only with a subset of those. Interestingly, all three of the nonneutralizing MAb sites were shared with at least one other serotype; the NN2 site was the most broadly cross-reactive.

Epitope-mapping studies. The antigenic sites on VP4 identified by this panel of MAbs was determined by using CMCE and IgG purified from ascites fluids. Each MAb was tested against the other 14 MAbs, as well as against itself, by using SA11 stock preparations. An anti-VP6 MAb (MAb 255) and virus incubated with buffer alone were included as internal controls. Competitive binding curves were subsequently generated, and MAbs were ultimately grouped on the basis of both their competition results and biological activities.

Analysis of typical competitive binding curves (Fig. 3) revealed that competition between MAbs could easily be determined by using this test format. In every case in which homologous MAb was used as the competitor MAb, a concentration-dependent competition effect was observed. Similarly, some heterologous MAbs also caused obvious competition, while others either had no effect or strongly enhanced binding. Competition curves were reproducible, and similar results were obtained when two separate hyperimmune guinea pig sera to double-shelled virus were used as detector antibodies.

The binding curves obtained using a nonneutralizing MAb (5E4) as the capture antibody (Fig. 3A and B) demonstrate all four types of reactivity (e.g., competition, partial competition, no competition, and enhancement of binding) seen with CMCE. When the homologous 5E4 MAb was used as the competitor MAb (shown in both panels), obvious competition occurred. Similar results were seen when 3C8 (Fig. 3A) or 2G4 (Fig. 3B) was the competing MAb. The 2G4 MAb competed with 5E4 and with all of the anti-VP4 MAbs tested (data not shown). No competition was seen with 5E4 and 3D8 (Fig. 3A) or 5E4 and 8D4 (Fig. 3B), or the anti-VP6 MAb, 255 (Fig. 3B), indicating that 5E4, 3D8, and 8D4 map to different antigenic sites.

An enhancement of binding was observed with 9F6 and 10G6 (Fig. 3A) and 7G6 and 8B6 (Fig. 3B). Similar binding enhancement was seen when any of the NP1 MAbs was used as the competing MAb with any of the nonneutralizing MAbs as the capture MAb. Partial competition (competition only at the highest concentration of competitor tested) was observed when the 954/23 MAb was used as the competitor MAb (Fig. 3A). 954/23 showed partial competition with all the anti-VP4 MAbs tested (data not shown).

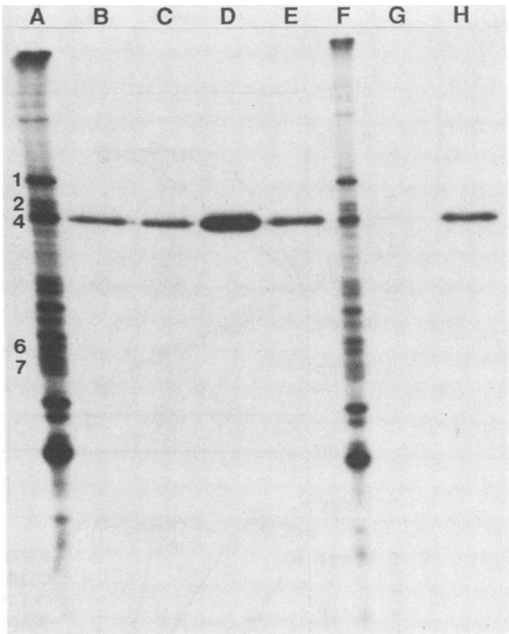

FIG. 2. Representative anti-SA11 MAbs from each antigenic site were analyzed in a direct SPIT. HPLC-purified immunoglobulin was bound directly to a polyvinyl chloride microplate. After blocking with BLOTTO, radiolabeled SA11 lysate was added. After removal of the lysate, the plates were washed, and samples were analyzed on a 10% polyacrylamide gel containing SDS. The gels were dried, and autoradiographs were prepared. Lanes A and F contain [^{35}S]methionine-labeled, SA11-infected cell lysates. Capture MAbs used were 3C8 (lane B), 7C6 (lane C), 5B10 (lane D), 3D8 (lane E), 9F6 (lane G), and 10G6 (lane H). Numbers at the left indicate the viral polypeptides, as designated by Estes et al. (16) and modified by Liu et al. (29a).

TABLE 2. Micro-IF reactivities of representative anti-VP4 MAbs with heterologous rotaviruses[a]

MAb	Antigenic site	Rotavirus strain tested (serotype)						
		Wa (1)	S2 (2)	SA11 (3)	Ito (3)	CU-1 (3)	St. Thomas 3 (4)	69M (8)
3C8	NN1	−	−	+	−	+	−	+
5B5	NN1	−	−	+	−	+	−	+
8D4	NN2	+	−	+	+	+	+	+
9E3	NN2	+	−	+	+	+	+	+
3D8	NN3	−	−	+	+	+	−	+
8B6	NP1a	−	−	+	+	−	−	−
9F6	NP1a	−	−	+	+	−	−	−
7G6	NP1b	−	−	+	+	+	−	−
10G6	NP1b	−	−	+	+	+	−	−
2G4	NP2	−	−	+	+	+	−	+
954/23	NP3	−	−	+	+	−	−	−

[a] Representative MAbs (two from each site with two or more MAbs mapping to it), at a concentration of 6 μg of HPLC-purified IgG per ml of PBS, were tested against infected MA104 cells in 96-well tissue culture plates. Results were determined independently by two observers using coded plates. Reactions with pooled mouse anti-SA11 hyperimmune serum (used as a positive control) gave strong positive results with each virus.

Figure 3C and D show the binding curves obtained using a neutralizing MAb (7G6) and another nonneutralizing MAb (9E3) as the capture antibodies. With 7G6 as the capture MAb (Fig. 3C), no enhanced binding was observed with any of the competing MAbs. With 9E3 as the capture MAb, enhanced binding was seen with an NP1 MAb (8B6) as the competitor MAb when compared with the anti-VP6 MAb 255 (Fig. 3D).

CMCE results for all the MAbs tested are summarized in Fig. 4. The three neutralization-negative sites, NN1 through NN3, were clearly separated by the CMCE binding curves, and all were subject to positive cooperative binding when an NP1 MAb was used as the capture MAb. The neutralization-positive site NP1 was further subdivided into sites NP1a (8B6 and 9F6) and NP1b (7G6 and 10G6) on the basis of differences in biological properties and CMCE reactivities.

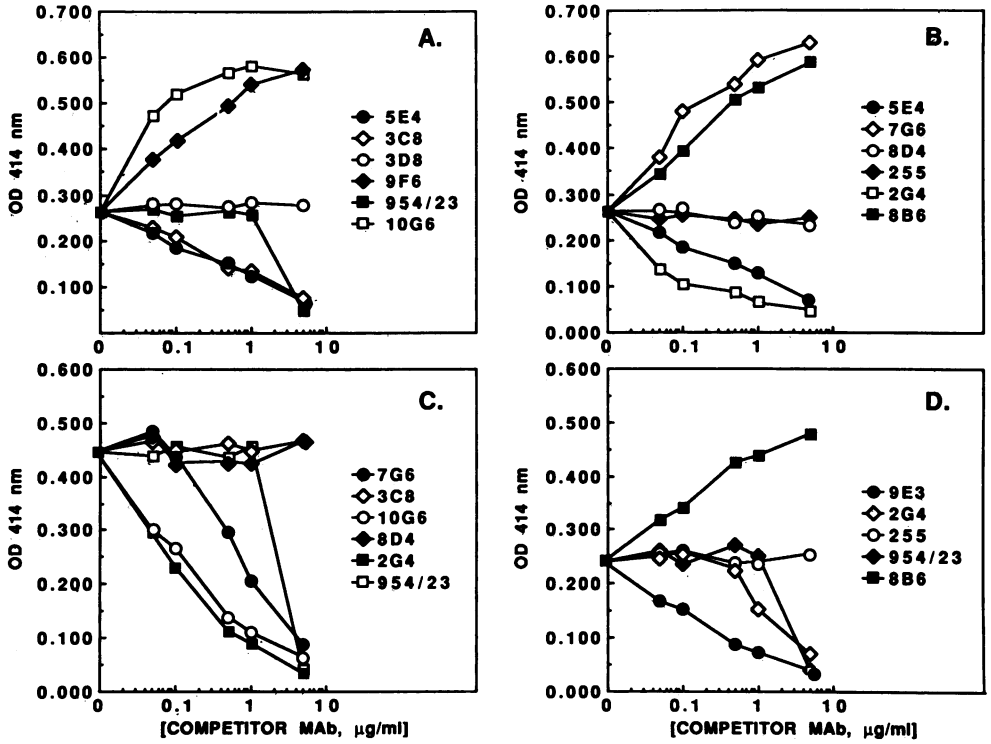

FIG. 3. Typical competitive binding curves generated from CMCE data. Increasing concentrations of purified competitor MAb (0.05, 0.1, 0.5, 1, and 5 μg/ml) were used to determine the extent of competition with a purified capture MAb bound to the wells of a microtiter plate (see Materials and Methods). The capture MAb was 5E4 in panels A and B, 7G6 in panel C, and 9E3 in panel D. Each point is the average of two tests. OD, Optical density.

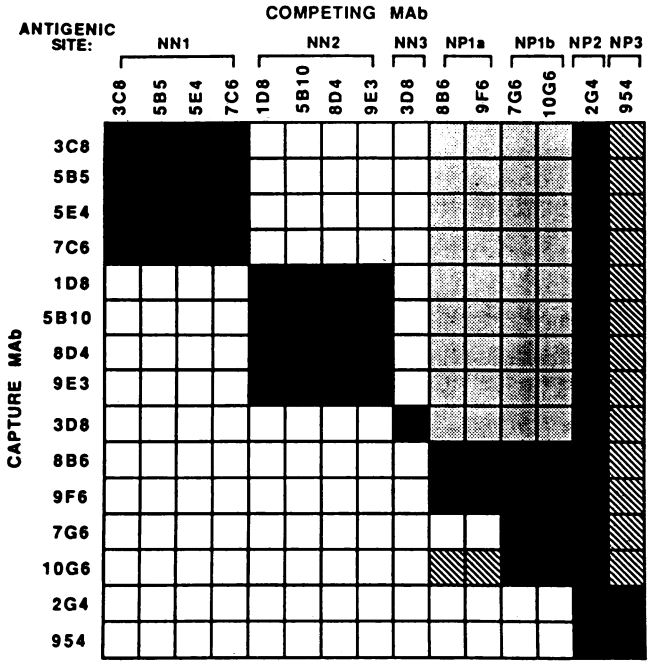

FIG. 4. Summary of epitope-mapping data. All 15 MAbs were mapped to epitopes by CMCE. Symbols for binding interactions between two MAbs: □, no competition; ▢, enhanced binding, defined as 50% increased binding with competitor MAb concentrations of 5 to 0.5 μg/ml; ■, competition, defined as 50% decreased binding with 5 μg/ml and 30% decrease with 1 μg of competitor MAb per ml; ▧, partial competition, defined as 50% decreased binding with 5 μg/ml or 30% decreased binding with 1 μg of competitor MAb per ml.

The NP1b MAbs were capable of competing with each other and with the NP1a MAbs. However, only a one-way competition was seen between NP1a MAbs and 7G6 (neither 8B6 nor 9F6 could compete with 7G6 as the capture MAb), and partial competition was seen between NP1a MAbs and 10G6 when 10G6 was used as the capture MAb. Finally, the PRN and HI endpoint titers (Table 1) support this subdivision, as the NP1a MAbs have lower titers than the NP1b MAbs in both assays.

MAbs 2G4 and 954/23 showed reciprocal competition with each other (40; data not shown). In spite of this, the epitopes recognized by the 2G4 and 954/23 MAbs were separated into two different sites, NP2 and NP3, for the following reasons. When used as a competitor, 954/23 caused only partial competition with the NN1 through NN3 and NP1 MAbs, while MAb 2G4 usually outcompeted any of the heterologous MAbs used for capture. No other MAb showed competition when either 954/23 or 2G4 was the capture MAb. In addition, these two MAbs were distinguishable by their different reactivities in the micro-IF test (Table 2) and they have been mapped to different cleavage products of VP4 (31).

Effect of trypsin on MAb binding. During the epitope-mapping experiments, it became apparent that some MAbs bound virus propagated in the absence of trypsin less effectively. This phenomenon was observed with all but one (3D8) of the nonneutralizing MAbs. This differential binding was not seen with any of the neutralizing anti-VP4 MAbs tested.

This observation was investigated further by examining the ability of trypsin-treated virus to be bound by the different capture MAbs in the MCE. In these experiments, two samples of a stock of SA11 generated in the absence of trypsin were prepared, and trypsin (8 μg/ml) was added to one sample while PBS was added to the second sample. After incubation at 37°C for 30 min, aprotinin was added to each tube to inhibit further protease activity. The tubes were then placed at 4°C, and these preparations were used as antigens in MCE. Those MAbs mapping to nonneutralizing epitopes bound trypsin-treated virus more efficiently than the identical non-trypsin-treated preparations (Table 3). In contrast, the neutralizing MAbs appeared to bind both preparations equally well. This finding was reproducible and occurred in every MCE in which a nonneutralizing MAb was used for the capture of non-trypsin-treated virus preparations.

DISCUSSION

The rotavirus outer capsid protein VP4 possesses several biologically significant properties in addition to hemagglutination. Studies using rotavirus reassortants have shown the following: (i) that neutralization phenotype segregates with either gene 4 or gene 9, which code for VP4 and VP7, respectively (23, 35, 37), (ii) that VP4 is as important as VP7 in the generation of neutralizing antibodies (22, 23), and (iii) that virulence is a property of gene segment 4 (36). Finally, studies of the nucleotide sequence of gene 4 from rotavirus strains isolated from neonates with either symptomatic or asymptomatic infections provide indirect evidence that the cleavage properties of VP4 may be correlated with the outcome of infections (17). Such data make it increasingly clear that VP4 plays a significant role in pathogenesis and recovery from rotavirus-induced disease and suggest that attempts to produce rotavirus subunit vaccines should include VP4 (1, 12, 31). Knowledge of the epitopes of VP4 identified through immunochemical analyses with MAbs should further our understanding of the functions and signif-

TABLE 3. Effect of trypsin treatment of virus on MAb binding

MAb	Epitope	OD_{414} in MCE of virus[a]		% Binding after trypsin treatment[b]
		Without trypsin	With trypsin (8 μg/ml)	
3C8	NN1	0.183	0.294	161
5B5	NN1	0.219	0.335	153
5E4	NN1	0.152	0.236	155
7C6	NN1	0.226	0.321	142
1D8	NN2	0.203	0.335	165
5B10	NN2	0.184	0.335	182
8D4	NN2	0.112	0.242	216
9E3	NN2	0.156	0.273	175
3D8	NN3	0.169	0.209	124
8B6	NP1a	0.306	0.333	108
9F6	NP1a	0.312	0.311	99
7G6	NP1b	0.360	0.322	89
10G6	NP1b	0.280	0.254	91
2G4	NP2	0.565	0.699	124
954	NP3	0.380	0.390	102

[a] Samples of the same crude SA11 virus preparation, generated in the absence of trypsin, were incubated at 37°C for 30 min in either the presence or absence of trypsin as described in Materials and Methods. These preparations were then used in the MCE. The optical density (OD) values shown represent the average of three tests (minus the value obtained by using MA104 crude preparations as a negative control for nonspecific binding).

[b] The percent binding after trypsin treatment was calculated for a given capture MAb as follows: (OD_{414} of trypsin-treated virus binding/OD_{414} of non-trypsin-treated virus binding) × 100, where OD_{414} is the optical density at 414 nm.

icance of this molecule. This paper describes the first antigenic analysis of VP4 on SA11.

The SA11 VP4 MAbs used in this study were generated and characterized by a different strategy from that used by previous workers. First, to enhance the chances of generating anti-VP4 clones, we used a mixture of purified double-shelled particles and soluble proteins isolated from the top fraction of CsCl gradients as our immunogen. These fractions were found to be greatly enriched in VP4 (34; R. F. Ramig, personal communication). In contrast to most previous studies, in which anti-VP4 and anti-VP7 hybridomas were identified by using either HI (19, 28, 40) or fluorescent-focus neutralization assays (43, 44), we used a micro-IF assay, similar to that of Roseto et al. (39), to screen our hybridomas. This procedure avoided the selection of MAbs with only one specific biological property, and we obtained MAbs to VP2, VP4, VP6, and VP7. To identify anti-VP4 hybridomas for the present study, we used a SPIT in addition to radioimmunoprecipitation. This allowed us to determine the specificity of some hybridomas that otherwise would not have been identified. Our combined procedures were effective in selecting a large number of both neutralizing and nonneutralizing MAbs that identify epitopes not previously described on VP4.

The combined results from our epitope mapping studies and biological assays indicate the presence of six antigenic sites on SA11 VP4. The epitope mapping studies were accomplished, and greatly facilitated by, use of the CMCE. This assay has a number of inherent advantages over the more conventional competitive binding ELISA. Traditional procedures, e.g., biotinylation or labeling of MAbs with enzymes or radioisotopes, are very time consuming. The entire panel of MAbs must be labeled and then standardized on the basis of the relative specific activities of the MAbs. Further, direct labeling of the MAbs may result in the loss of their antigen-binding activity (24). Our procedure (modified from Hendry et al. [20]) allows the investigator to use commercially available labeled reagents and crude antigen preparations without further purification. This procedure requires that limiting antigen conditions be used to provide maximum sensitivity. To achieve this, the antigen preparation is diluted and therefore can be used for a greater number of assays. Finally, the more traditional mapping procedure first binds virus to the plate either directly or through a capture antibody. Virus that has been purified and bound directly to a plate with a buffer at high pH (i.e., bicarbonate buffer [pH 9.6]) may lose reactivity with some MAbs (32, 45). For example, our NP1 MAbs are unable to bind efficiently to virus bound directly to plates (J. W. Burns and M. K. Estes, unpublished observation). In the CMCE procedure, the MAbs bind virus in solution, allowing virus particles to maintain their native structure and the flexibility to undergo normal conformational changes following virus-antibody interactions. These observations indicate that CMCE is not only a rapid epitope-mapping procedure but may also provide useful and complementary information not obtained using the more traditional technique.

It is of interest to compare our six SA11 antigenic sites with those reported on VP4 by others (40, 43). Three of the SA11 sites are involved in neutralization (neutralization positive, NP1 through NP3) and three are not critical for neutralization (neutralization negative, NN1 through NN3). Three antigenic sites (two of which were neutralizing) have been described for VP4 of RRV (3A, 3B, and 3C; 40), and three cross-reactive neutralization epitopes have been identified on some human rotaviruses (43). Our SA11 neutralization-negative MAbs (NN1 and NN3) would not have been detected by Shaw et al. (40) or Taniguchi et al. (44) as a result of their lack of HI and neutralizing activity. In contrast, our NN2 epitope, which contains nonneutralizing MAbs with low levels of HI activity, may correspond to the one nonneutralizing epitope identified on RRV (3C).

Neutralizing MAbs comparable with our NP1 site were not identified by Shaw et al. (40), possibly because of the different methods used for MAb screening and characterization (see above). Our SA11 NP2 site is the RRV 3B epitope identified by MAb 2G4. This is a cross-reactive neutralization site located in VP5 (31) and identical to one (site II marked by MAbs KU-6B11, YO-1E6, YO-153, and ST-1F2) of the three neutralization sites identified on human rotaviruses (43; K. Taniguchi, M. Gorziglia, Y. Morita, T. Urasawa, S. Urasawa, A. Z. Kapikian, and R. M. Chanock, Abstr. 7th Intl. Congr. Virol. 1987, R11.54, p. 117). The SA11 NP3 site is the same as the 3A epitope on RRV. This site (RRV 3A) has been localized on VP8, and it is composed of mostly strain-specific MAbs, except for 954/23 (called 23 by Shaw et al. [40]). We and Taniguchi et al. (Taniguchi et al., 7th Intl. Congr. Virol. 1987) did not generate hybridomas reactive with NP3.

A previously unreported observation from our epitope-mapping studies is that conformational changes apparently occur as a result of the binding of some neutralizing VP4 MAbs to virus particles. This causes an increase in the ability of the NN1 through NN3 capture MAbs to bind VP4 when NP1 MAbs are used as the competitor. This binding enhancement could be due either to an increase in the accessibility of the epitope or to the exposure of a greater number of epitopes. Enhanced binding with two neutralizing rotavirus VP7 MAbs has also been reported by Shaw et al. (40) with the suggestion that one of these anti-VP7 MAbs might cause a conformational change in the virus structure. Because all of the anti-VP4 MAbs described here that appear to induce conformational changes also neutralize viral infectivity, such changes in virion structure may be detrimental to infectivity and could be the basis of neutralization. Crystallographic data for the binding of antibody to influenza virus particles and biochemical studies with other viruses support antibody-induced conformational changes as one possible mechanism of virus neutralization (5, 8, 10, 30). However, direct proof of the mechanism(s) of rotavirus neutralization after reactivity with different neutralizing MAbs requires additional study.

Our observation that the neutralization-negative MAbs react more strongly with trypsin-treated virus suggests these sites may have an increased surface exposure after proteolysis. In contrast to these results, several nonneutralizing anti-VP7 MAbs generated to a human rotavirus and cross-reactive with SA11 show decreased binding to trypsin-treated virus (7). These results, taken together, suggest that in the process of increasing viral infectivity, trypsin treatment may alter the accessibility or conformation of several epitopes on the outer capsid proteins.

On the basis of the data reported here, we suggest a possible topographic map for VP4 of SA11 (Fig. 5). This map is also consistent with the existing data on the hemagglutinins of RRV-2 and human rotavirus (28, 40, 44). Currently, we cannot determine if the neutralization and hemagglutination epitopes lie in separate domains or if they are all located in a large neutralization or hemagglutination domain. For simplicity, we have assumed that all these epitopes are contained within larger domains, although this may not be the case. The three neutralizing sites appear to lie within the

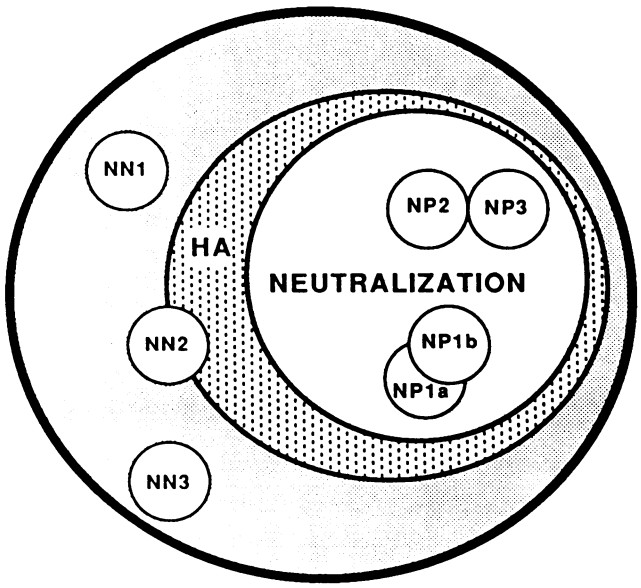

FIG. 5. Proposed map of the antigenic sites on the SA11 hemagglutinin. Map of the antigenic sites on VP4 showing the six sites described. For simplicity, we have shown one large neutralization domain, containing all of the neutralization sites, within a large HA domain.

hemagglutination domain, because they all have HI activity, but not all HI-positive MAbs can neutralize. The NN2 site partially overlaps the hemagglutination domain, because two of the four MAbs defining this epitope (1D8 and 5B10) are not able to inhibit hemagglutination while the remaining two MAbs do have HI activity. We have not yet identified which cleavage product of VP4 our MAbs react with, but the NP2 and NP3 MAbs have been shown to reside on VP5* and VP8*, respectively, for RRV (31). Therefore, neutralization and HA domains for SA11 must reside on both these cleavage products. This contrasts with the report that the HA domain for a human rotavirus strain resides on VP8 (28). Antigenic sites NN1 and NN3 appear to be located elsewhere on the molecule, as they display neither neutralization nor HI activity. The availability of other anti-VP4 MAbs reactive with SA11 and sequence analysis of neutralization escape mutants selected with our NP1 neutralizing MAbs will allow a more accurate mapping of those regions of VP4 involved in neutralization.

ACKNOWLEDGMENTS

This work was supported in part by Public Health Service grants DK-30144 from the National Institute of Arthritis, Diabetes, and Digestive and Kidney Diseases and AI-20649 from the National Institute of Allergy and Infectious Diseases, by National Research Service award CA-09197, and by Public Health Service grant RR-05425.

We thank Frank Ramig for helpful suggestions throughout the study.

LITERATURE CITED

1. **Arias, C. F., M. Lizano, and S. Lopez.** 1987. Synthesis in *Escherichia coli* and immunological characterization of a polypeptide containing the cleavage sites associated with trypsin enhancement of rotavirus SA11 infectivity. J. Gen. Virol. **68**:633–642.
2. **Bradford, M. M.** 1976. A rapid and sensitive method for the quantitation of microgram quantities of protein utilizing the principle of protein-dye binding. Anal. Biochem. **72**:248–254.
3. **Brodeur, B. R., P. Tsang, and Y. Larose.** 1984. Parameters affecting ascites tumour formation in mice and monoclonal antibody production. J. Immunol. Methods **71**:265–272.
4. **Chan, W.-K., M. E. Penaranda, S. E. Crawford, and M. K. Estes.** 1986. Two glycoproteins are produced from the rotavirus neutralization gene. Virology **151**:243–252.
5. **Colman, P. M., W. G. Laver, J. N. Varghese, A. T. Baker, P. A. Tulloch, G. M. Air, and R. G. Webster.** 1987. Three-dimensional structure of a complex of antibody with influenza virus neuraminidase. Nature (London) **326**:358–363.
6. **Coulson, B. S., K. J. Fowler, R. F. Bishop, and R. G. H. Cotton.** 1985. Neutralizing monoclonal antibodies to human rotavirus and indications of antigenic drift among strains from neonates. J. Virol. **54**:14–20.
7. **Coulson, B. S., K. J. Fowler, J. R. White, and R. G. H. Cotton.** 1987. Nonneutralizing monoclonal antibodies to a trypsin sensitive site on the major glycoprotein of rotavirus which discriminate between virus serotypes. Arch. Virol. **93**:199–211.
8. **Dimmock, N. J.** 1984. Mechanisms of neutralization of animal viruses. J. Gen. Virol. **65**:1015–1022.
9. **Echeverria, P., N. R. Blacklow, G. G. Cukor, S. Vibulbandhitkit, S. Changchawalit, and P. Boonthai.** 1983. Rotavirus as a cause of severe gastroenteritis in adults. J. Clin. Microbiol. **18**:663–667.
10. **Emini, E. A., P. Ostapchuk, and E. Wimmer.** 1983. Bivalent attachment of antibody onto poliovirus leads to conformational alteration and neutralization. J. Virol. **48**:547–550.
11. **Espejo, R. T., S. López, and C. Arias.** 1981. Structural polypeptides of simian rotavirus SA11 and the effect of trypsin. J. Virol. **37**:156–160.
12. **Estes, M. K., S. E. Crawford, M. E. Penaranda, B. L. Petrie, J. W. Burns, W.-K. Chan, B. Ericson, G. E. Smith, and M. D. Summers.** 1987. Synthesis and immunogenicity of the rotavirus major capsid antigen using a baculovirus expression system. J. Virol. **61**:1488–1494.
13. **Estes, M. K., and D. Y. Graham.** 1980. Identification of rotaviruses of different origins by the plaque-reduction test. Am. J. Vet. Res. **41**:151–152.
14. **Estes, M. K., D. Y. Graham, and B. B. Mason.** 1981. Proteolytic enhancement of rotavirus infectivity: molecular mechanisms. J. Virol. **39**:879–888.
15. **Estes, M. K., D. Y. Graham, and B. L. Petrie.** 1985. Antigenic structure of rotaviruses, p. 389–405. *In* M. H. V. van Regenmortel and A. R. Neurath (ed.), Immunochemistry of viruses: the basis for serodiagnosis and vaccines. Elsevier Science Publishers, Amsterdam.
16. **Estes, M. K., E. L. Palmer, and J. F. Obijeski.** 1983. Rotaviruses: a review. Curr. Top. Microbiol. Immunol. **105**:123–184.
17. **Gorziglia, M., Y. Hoshino, A. Buckler-White, I. Blumentals, R. Glass, J. Flores, A. Z. Kapikian, and R. M. Chanock.** 1986. Conservation of amino acid sequence of VP8 and cleavage region of 84-kDa outer capsid protein among rotaviruses recovered from asymptomatic neonatal infection. Proc. Natl. Acad. Sci. USA **83**:7039–7043.
18. **Greenberg, H. B., J. Flores, A. R. Kalica, R. G. Wyatt, and R. G. Jones.** 1983. Gene coding assignments for growth restriction, neutralization and subgroup specificities of the W and DS-1 strains of human rotavirus. J. Gen. Virol. **64**:313–320.
19. **Greenberg, H. B., J. Valdesuso, K. Van Wyke, K. Midthun, M. Walsh, V. McAuliffe, R. G. Wyatt, A. R. Kalica, J. Flores, and Y. Hoshino.** 1983. Production and preliminary characterization of monoclonal antibodies directed at two surface proteins of rhesus rotavirus. J. Virol. **47**:267–275.
20. **Hendry, R. M., B. F. Fernie, L. J. Anderson, E. Godfrey, and K. McIntosh.** 1985. Monoclonal capture antibody ELISA for respiratory syncytial virus: detection of individual viral antigens and determination of monoclonal antibody specificities. J. Immunol. Methods **77**:247–258.
21. **Holmes, I. H.** 1983. Rotavirus, p. 359–423. *In* W. K. Joklik (ed.), The Reoviridae. Plenum Publishing Corp., New York.
22. **Hoshino, Y., M. M. Sereno, K. Midthun, J. Flores, R. M. Chanock, and A. Z. Kapikian.** 1987. Analysis by plaque reduction neutralization assay of intertypic rotaviruses suggests that

gene reassortment occurs in vivo. J. Clin. Microbiol. **25**:290–294.
23. **Hoshino, Y., M. M. Sereno, K. Midthun, J. Flores, A. Z. Kapikian, and R. M. Chanock.** 1985. Independent segregation of two antigenic specificities (VP3 and VP7) involved in neutralization of rotavirus infectivity. Proc. Natl. Acad. Sci. USA **82**: 8701–8704.
24. **Howard, C. R., H. Lewicki, L. Allison, M. Salter, and M. J. Buchmeier.** 1985. Properties and characterization of monoclonal antibodies to Tacaribe virus. J. Gen. Virol. **66**:1383–1395.
25. **Hrdy, D. B.** 1987. Epidemiology of rotaviral infection in adults. Rev. Infect. Dis. **9**:461–469.
26. **Hung, T., G. Chen, C. Wang, H. Yao, Z. Fang, T. Chao, Z. Chou, W. Ye, X. Chang, S. Den, X. Liong, and W. Chang.** 1984. Waterborne outbreak of rotavirus diarrhoea in adults in China caused by a novel rotavirus. Lancet **i**:1139–1142.
27. **Johnson, D. A., J. W. Gautsch, J. R. Sportsman, and J. H. Elder.** 1984. Improved technique utilizing nonfat dry milk for analysis of proteins and nucleic acids transferred to nitrocellulose. Gene Anal. Tech. **1**:3–8.
28. **Kitaoka, S., M. Fukuhara, F. Tazawa, H. Suzuki, T. Sato, T. Konno, T. Ebina, and N. Ishida.** 1986. Characterization of monoclonal antibodies against human rotavirus hemagglutinin. J. Med. Virol. **19**:313–323.
29. **Lane, R. D., R. S. Crissman, and M. F. Lachman.** 1984. Comparison of polyethylene glycols as fusogens for producing lymphocyte-myeloma hybrids. J. Immunol. Methods **72**:71–76.
29a. **Liu, M., P. A. Offit, and M. K. Estes.** 1988. Identification of the simian rotavirus SA11 genome segment 3 product. Virology **163**:26–32.
30. **Lubeck, M. D., and W. Gerhard.** 1981. Topological mapping of the antigenic sites on the influenza A/PR/8/34 virus hemagglutinin using monoclonal antibodies. Virology **113**:64–72.
31. **Mackow, E. R., R. D. Shaw, S. M. Matsui, P. T. Vo., M. N. Ngoc, and H. B. Greenberg.** 1988. The rhesus rotavirus gene encoding protein VP3: location of amino acids involved in homologous and heterologous rotavirus neutralization and identification of a putative fusion region. Proc. Natl. Acad. Sci. USA **85**:645–649.
32. **Najjar, J. A., J. R. Gentsch, N. Nathanson, and F. Gonzalez-Scarano.** 1985. Epitopes of the G1 glycoprotein of La Crosse virus form overlapping clusters within a single antigenic site. Virology **144**:426–432.
33. **Nau, D. R.** 1986. A unique chromatographic matrix for rapid antibody purification. Biochromatography **1**:82–94.
34. **Novo, E., and J. Esparza.** 1981. Composition and topography of structural polypeptides of bovine rotavirus. J. Gen. Virol. **56**: 325–335.
35. **Offit, P. A., and G. Blavat.** 1986. Identification of the two rotavirus genes determining neutralization specificities. J. Virol. **57**:376–378.
36. **Offit, P. A., G. Blavat, H. B. Greenberg, and H. F. Clark.** 1986. Molecular basis of rotavirus virulence: role of gene segment 4. J. Virol. **57**:46–49.
37. **Offit, P. A., H. F. Clark, G. Blavat, and H. B. Greenberg.** 1986. Reassortant rotaviruses containing structural proteins vp3 and vp7 from different parents induce antibodies protective against each parental serotype. J. Virol. **60**:491–496.
38. **Offit, P. A., R. D. Shaw, and H. B. Greenberg.** 1986. Passive protection against rotavirus-induced diarrhea by monoclonal antibodies to vp3 and vp7. J. Virol. **58**:700–703.
39. **Roseto, A., R. Scherrer, J. Cohen, M. C. Guillemin, A. Charpilienne, C. Feynerol, and J. Peries.** 1983. Isolation and characterization of anti-rotavirus immunoglobulins secreted by cloned hybridoma cell lines. J. Gen. Virol. **64**:237–240.
40. **Shaw, R. D., P. T. Vo, P. A. Offit, B. S. Coulson, and H. B. Greenberg.** 1986. Antigenic mapping of the surface proteins of rhesus rotavirus. Virology **155**:434–451.
41. **Sonza, S., A. M. Breschkin, and I. H. Holmes.** 1984. The major surface glycoprotein of simian rotavirus (SA11) contains distinct epitopes. Virology **134**:318–327.
42. **Tamura, G. S., M. O. Dailey, W. M. Gallatin, M. S. McGrath, I. L. Weissman, and E. A. Pillemer.** 1984. Isolation of molecules recognized by monoclonal antibodies and antisera: the solid phase immunoisolation technique (SPIT). Anal. Biochem. **136**: 458–464.
43. **Taniguchi, K., Y. Morita, T. Urasawa, and S. Urasawa.** 1987. Cross-reactive neutralization epitopes on VP3 of human rotavirus: analysis with monoclonal antibodies and antigenic variants. J. Virol. **61**:1726–1730.
44. **Taniguchi, K., S. Urasawa, and T. Urasawa.** 1985. Preparation and characterization of neutralizing monoclonal antibodies with different reactivity patterns to human rotaviruses. J. Gen. Virol. **66**:1045–1053.
45. **Tremaine, J. H., W. P. Ronald, and D. J. MacKenzie.** 1985. Southern bean mosaic virus monoclonal antibodies: reactivity with virus strains and with the virus antigen in different conformations. Phytopathology **75**:1208–1211.